Journal of Affective Disorders 207 (2017) 18–25

Contents lists available at ScienceDirect

Journal of Affective Disorders

journal homepage: www.elsevier.com/locate/jad

DTI-based connectome analysis of adolescents with major depressive disorder reveals hypoconnectivity of the right caudate

Olga Tymofiyeva [a,*], Colm G. Connolly [b], Tiffany C. Ho [b,c], Matthew D. Sacchet [b,c], Eva Henje Blom [b,d], Kaja Z. LeWinn [b], Duan Xu [a], Tony T. Yang [b]

[a] Department of Radiology and Biomedical Imaging, University of California San Francisco, United States
[b] Department of Psychiatry, University of California San Francisco, United States
[c] Department of Psychology and Neurosciences Program, Stanford University, United States
[d] Department of Clinical Neuroscience, Karolinska Institute, Sweden

ARTICLE INFO

Article history:
Received 12 April 2016
Accepted 18 September 2016
Available online 19 September 2016

Keywords:
MRI
Adolescence
Brain
Depression
Diffusion
Tractography
Connectomics
Graph theory
Neural network
Caudate

ABSTRACT

Background: Adolescence is a vulnerable period for the onset of major depressive disorder (MDD). While some studies have shown white matter alterations in adolescent MDD, there is still a gap in understanding how the brain is affected at a network level.
Methods: We compared diffusion tensor imaging (DTI)-based brain networks in a cohort of 57 adolescents with MDD and 41 well-matched healthy controls who completed self-reports of depression symptoms and stressful life events. Using atlas-based brain regions as network nodes and tractography streamline count or mean fractional anisotropy (FA) as edge weights, we examined weighted local and global network properties and performed Network-Based Statistic (NBS) analysis.
Results: While there were no significant group differences in the global network properties, the FA-weighted node strength of the right caudate was significantly lower in depressed adolescents and correlated positively with age across both groups. The NBS analysis revealed a cluster of lower FA-based connectivity in depressed subjects centered on the right caudate, including connections to frontal gyri, insula, and anterior cingulate. Within this cluster, the most robust difference between groups was the connection between the right caudate and middle frontal gyrus. This connection showed a significant diagnosis by stress interaction and a negative correlation with total stress in depressed adolescents.
Limitations: Use of DTI-based tractography, one atlas-based parcellation, and FA values to characterize brain networks represent this study's limitations.
Conclusions: Our results allowed us to suggest caudate-centric models of dysfunctional processes underlying adolescent depression, which might guide future studies and help better understand and treat this disorder.

1. Introduction

According to the World Health Organization (WHO), major depressive disorder (MDD) is the current leading cause of disability worldwide and adolescence is a vulnerable period for onset of depression, affecting more than 10% of adolescents in the US (SAMHSA, 2014). Depressed adolescents are at higher risk of suicide, which is the second leading cause of death for young people ages 15–34, according to the National Institute for Mental Health (NIMH). Apart from this most devastating outcome, depressed teens are facing other negative health outcomes including substance use disorder and physical health problems, and early onset MDD predicts a four-fold increase in the risk of developing adult depression (Naicker et al., 2013). Uncovering the neurobiological basis of adolescent MDD, which might differ from the adult form, is essential for the development of much needed effective treatment paradigms, since the effectiveness of current psychological interventions, antidepressant medication and a combination of these interventions for treating depressive disorders in children and adolescents has not been fully established (Cox et al., 2014).

Adolescence is a period of ongoing myelination and brain network development (Casey et al., 2008). While some studies have shown white matter alterations in adolescent MDD, located primarily in the frontolimbic areas (Cullen et al., 2010; Bessette et al., 2013; LeWinn et al., 2014), there is still a gap in understanding how the brain is affected at a network level. The recent explosive growth of connectome studies highlights the importance

* Correspondence to: Department of Radiology & Biomedical Imaging, University of California, San Francisco, 1700 4th St., Byers Hall Suite 102, San Francisco, CA 94158, United States.
E-mail address: Olga.Tymofiyeva@ucsf.edu (O. Tymofiyeva).

http://dx.doi.org/10.1016/j.jad.2016.09.013
0165-0327/

Table 1
Demographic and clinical characteristics of the study participants.

Characteristic	MDD[a]	HC[a]	Statistic[b,c]	p value	Effect size (95% CI)	Signif.
Number of participants in final analysis (n)	57	41	$\chi2(1.00)=2.30$	0.13		
Gender (M/F)	24/33	16/25	$\chi2(1.00)=0.01$	0.92		
Age at time of scan (years)	16.2 ± 1.3 (13.1–17.9)	16 ± 1.4 (13.2–17.9)	t(82.92)=0.81	0.42	g=0.16 (−0.24; 0.57)	
Hollingshead Socioeconomic Score	40 ± 39 (11–73)†	29 ± 29 (0–77)†	W=1346	0.2	PS=0.395 (0.29; 0.51)	
Tanner Score	4.5 ± 0.5 (3–5)†	4 ± 0.5 (3–5)†	W=1433	0.05	PS=0.261 (0.17; 0.37)	*
Wechsler Abbreviated Scale of Intelligence	104.1 ± 22.4 (77–209)	107.3 ± 19.9 (74–204)	t(91.87)=−0.75	0.46	g=−0.15 (−0.56; 0.25)	
Children's Depression Rating Scale (Standardized)	72.5 ± 8.3 (55–85)	34.5 ± 6.9 (30–61)	t(93.69)=24.68	0	g=5.01 (4.20; 5.83)	***
Reynolds Adolescent Depression Scale Dysphoric Mood (Standardized)	63.4 ± 8.4 (35–78)	44.4 ± 9.5 (31–63) [1]	t(77.09)=10.15	0	g=2.06 (1.56; 2.56)	***
Reynolds Adolescent Depression Scale Anhedonia/Negative Affect (Standardized)	55.9 ± 11.1 (15–73)	45.1 ± 6.3 (40–71) [1]	t(91.34)=6.06	0	g=1.23 (0.79; 1.67)	***
Reynolds Adolescent Depression Scale Negative Self-evaluation (Standardized)	65.5 ± 9.1 (39–83)	45.9 ± 7.8 (39–64) [1]	t(90.95)=11.35	0	g=2.31 (1.79; 2.83)	***
Reynolds Adolescent Depression Scale Somatic Complaints (Standardized)	62.1 ± 7.3 (42–74)	42.5 ± 8.6 (29–67) [1]	t(75.32)=11.71	0	g=2.38 (1.85; 2.90)	***
Reynolds Adolescent Depression Scale Total (Standardized)	65.9 ± 8.3 (35–80)	42.9 ± 8.2 (30–64) [1]	t(84.75)=13.54	0	g=2.75 (2.19; 3.31)	***
Multidimensional Anxiety Scale for Children (Standardized)	59.7 ± 10.5 (32–78) [2]	42.1 ± 8.9 (26–61) [2]	t(89.20)=8.77	0	g=1.78 (1.31; 2.26)	***

Abbreviations: MDD, Major depressive disorder; HC, healthy control; M, male; F, female. CI, Confidence Interval; SD, standard deviation; g, Hedge's g.

[a] Mean ± SD (min–max) or median ± interquartile range (min–max) if indicated by †. The optional number in [] indicated the number of missing data points.

[b] Statistic: W, Wilcox rank sum test; χ^2, χ^2 test for equality of proportions; *t*, Student's *t* test.

[c] Statistics for clinical scales refer only to participants included in the final analysis.

* $p < 0.05$.

*** $p < 0.001$.

of this approach to viewing the brain's structure, at both microscopic and macroscopic levels (Sporns et al., 2005). Diffusion MRI has made it possible to image the macroscopic human brain connectome noninvasively and subsequently analyze it using graph theory, a mathematical framework for studying networks (Hagmann et al., 2007). MRI connectomics has already been successfully applied to studying brain network development (Tymofiyeva et al., 2014) and disruption in many neurological and psychiatric disorders (Griffa et al., 2013). The benefit of this approach in the study of depression is the potential of revealing topological disruptions of the brain's communication pathways in network space as opposed to purely anatomical space.

Recently, a preliminary study of 16 adolescents diagnosed with MDD and 16 healthy controls applied graph theory to examine resting-state functional connectivity (Jin et al., 2011). Their results include MDD-related decreases in the global graph metric of small-worldness, which indicates interconnectedness of both nearby and distant nodes of the network, and widespread increases in the local graph metric of node degree (i.e., the number of connections of a region). However, there have been no studies of the structural connectome in this population.

The goal of this study was to perform DTI-based connectome analysis in a cohort of depressed adolescents and well-matched non-depressed controls. Based on the literature, we hypothesized the following:

1) There will be differences in global and/or local network measures between adolescents with MDD and healthy controls.
2) The differences in local network measures, if present, will involve frontolimbic connections.
3) The differences in network measures, if present, will correlate with the depression severity scores.

As implied above, the comparison of connectomes can be undertaken on a global or a local (at the node or edge) level, which represent two complementary ways of analysis, allowing to assess differences in summary measures as well as local phenomena (Meskaldji et al., 2013). Comparison at a local level is associated with massive multiple comparisons problem, which can be effectively addressed by the Network-Based Statistic (NBS) approach (Zalesky et al., 2010). In our study we utilized both, global graph metrics, local graph metrics at the level of individual nodes, and the NBS for edge-wise comparison of connectomes.

Given the continuing maturation of white matter fibers throughout adolescence (Asato et al., 2010), as well as the role life stress plays in adolescent MDD (Auerbach et al., 2014), we also explored age and self-reported stressful life events as independent variables in our analyses.

2. Methods

2.1. Participants and clinical information

The Institutional Review Boards at the University of California San Diego, University of California San Francisco, Rady Children's Hospital in San Diego, and the County of San Diego approved this study. All participants in the study provided written informed assent and their parent(s) or legal guardian(s) provided written informed consent in accordance with the Declaration of Helsinki.

The study protocol, recruitment procedures, clinical and diagnostic assessments, and inclusion/exclusion criteria have been previously described (LeWinn et al., 2014). Data from 57 adolescents with MDD (age at time of scan 16.2 ± 1.3 (13.1–17.9), 33 females) and 41 well-matched healthy controls (HC) (age at time of scan 16 ± 1.4 (13.2–17.9), 25 females) were included in this study. Fifty-one MDD and 39 HC subjects overlapped with the study by LeWinn et al. (2014). Ten of the depressed subjects were medicated and 41 were medication-naïve. The MDD and HC groups were matched on age, gender, pubertal stage, and socioeconomic status. Details about the groups' characteristics can be found in Table 1.

For each participant, depression severity was assessed using both a clinician-rating scale, the Children's Depression Rating Scale-Revised (CDRS-R) (Poznanski and Mokros, 1996), and a self-report

scale, the Reynolds Adolescent Depression Scale (RADS-2) (Reynolds, 2002). The CDRS-R scores were used to further characterize study groups: controls with scores higher than 54 and MDD participants with scores lower than 55 were excluded. The RADS-2 scores were used in the present study for correlation analyses. Given the frequency of comorbid anxiety in adolescent depression, we also assessed anxiety symptoms with the Multidimensional Anxiety Scale for Children (MASC) (March et al., 1997). Total stress was assessed using the Stressful Life Events Schedule (Adolescent Self Report) (Williamson et al., 2003) by summing the severity of stressful life events that happened in the past six months.

2.2. MRI data acquisition

The data were collected using a 3T MRI system (MR750, GE Healthcare, Milwaukee, Wisconsin), Twin Speed gradients and an eight-channel head coil at the University of California San Diego Center for Functional Magnetic Resonance Imaging (CFMRI). High-resolution anatomical T1-weighted images were acquired using a fast spoiled gradient recalled (SPGR) pulse sequence (TR/TE = 8.1/3.17 ms, flip angle = 12°, slice thickness = 1 mm, FOV = 250 × 250 mm, 256 × 256 matrix, resulting in 0.98 × 0.98 × 1 mm voxels). The diffusion-weighted images were acquired using a dual spin echo, single-shot echo-planar imaging (EPI) sequence, 30 non-collinear directions, b-value 1500 s/mm^2, TR/TE = 7200/86.5 ms, FOV = 180 × 180 mm, 96 × 96 matrix, 1.875 × 1.875 × 2.5 mm voxels, 2 averages. Additionally, gradient echo field maps were acquired to compensate for magnetic field inhomogeneity using TR/TE1/TE2 = 1000/4.4/5.5 ms, flip angle = 12°, 128 × 128 matrix, 50 axial slices, 1.875 × 1.875 × 2.5 mm voxels.

2.3. MRI data preprocessing

The FMRIB Software Library (FSL; Smith et al., 2004) was used for preprocessing. The T1-weighted images were bias-field-corrected, skull-stripped, and transformed to MNI152 space using an affine transform. We used linear registration (FLIRT), since we did not expect strong atrophy in this population (Jenkinson et al., 2002). A quality assurance step was performed on DTI data as previously described (LeWinn et al., 2014), in which the data were field-map-corrected and outlier directions were removed. The data were transformed to NIFTI (Neuroimaging Informatics Technology Initiative) format. DTI reconstruction and deterministic whole-brain streamline fiber tractography were performed using the Diffusion Toolkit (Wang et al., 2007). For whole-brain tractography, the Fiber Assignment by Continuous Tracking (FACT) algorithm (Mori et al., 1999) with one seed per voxel was applied using the entire diffusion-weighted volume as the mask image. A threshold angle of 35° was chosen as a compromise between false positive and false negative streamlines (Moldrich et al., 2010).

2.4. Network construction and statistical analysis

Individual brains were segmented into 90 ROIs using the Automated Anatomical Labeling (AAL) atlas (Tzourio-Mazoyer et al., 2002). To achieve this, FA maps were transformed to T1-weighted images in MNI space using FLIRT and a transformation matrix *M* was obtained. After this, AAL labels were applied to DTI by inverting the matrix *M*. Visual assessment of the registration and segmentation result was satisfactory (see Supplementary Fig. S1). We chose the AAL atlas, since it is the most commonly used atlas for studying structural connectomics in brain disease (Griffa et al., 2013) and thus can facilitate comparison across studies. We excluded cerebellar regions, as is commonly done (Korgaonkar et al., 2014), therefore reducing the number of ROIs from 120 to 90. The ROIs were dilated by one voxel and used as network nodes. Connections between AAL ROIs were calculated using two methods: i) with the number of connecting streamlines (scaled by the total brain volume) serving as connection (edge) weights and ii) with the average FA along the streamlines serving as weights. Total brain volume was calculated as the sum of voxels of all included AAL ROIs multiplied by voxel volume. Only streamlines with at least 3 points were considered. The streamline-weighted and FA-weighted connections were stored as 90 × 90 connectivity matrices, in which each row/column corresponded to a distinct node (brain ROI).

2.4.1. Global and local graph metrics analyses

Using the Brain Connectivity Toolbox (Rubinov and Sporns, 2010), we examined weighted local and global network properties that are most commonly used in brain connectome analyses. The local property we investigated was *node strength* (the sum of weights of links connected to the node; equivalent of *node degree* for binary networks) and global properties included *average clustering coefficient* and *characteristic path length*, normalized by random networks. High *average clustering coefficient* represents high network segregation and high *characteristic path length* represents low network integration. We also analyzed *small-worldness*, which is computed as the ratio of these two metrics. General linear modeling (GLM) analyses were performed for the calculated network properties using diagnosis, age, and gender as independent variables. We adjusted the resulting *p*-values using the Bonferroni method.

2.4.2. Edge-based analyses

To assess edge-wise differences in the connectivity matrices between the two groups, we utilized the NBS approach (Zalesky et al., 2010). This process consists of four steps. The first step is to independently test the hypothesis of interest at every connection in the network with an appropriate statistical test (mass univariate testing). The second step is to choose a test statistic threshold, referred to as the primary threshold. The connections with a test statistic value exceeding this threshold are admitted to a set of supra-threshold connections. The third step is to identify topological clusters among the set of supra-threshold connections using a breadth or depth search. The presence of a component may provide evidence of a non-chance structure for which the null hypothesis can be rejected at the level of the structure as a whole, but not for any individual connection alone. The final step is to compute the family-wise error rate (FWER)-corrected p-value for each component using permutation testing. We specified the FWER-corrected significance level (alpha threshold) at the default value of 0.05. We performed a *t*-test with 5000 permutations and tested a range of primary thresholds (3.5, 3.6, 3.7… 6) in order to determine the highest threshold value at which the number of significantly different connections plateaued.

For the network properties that differed significantly between the groups and for the connection in the NBS-identified cluster with the highest t-value, we performed linear regression analyses to assess their association with the clinician-rated depression symptom severity (CDRS-R), self-reported depression symptom severity (RADS-2 and its subscales Dysphoric Mood, Anhedonia/Negative Affect, Negative Self-Evaluation, and Somatic Complaints), anxiety, and total stress scores.

The statistical analyses were performed using JMP software (version 12.0.1; SAS Institute, Cary, NC, USA).

3. Results

The MDD and HC adolescent groups showed expected significant differences in levels of depression and anxiety on all scales (CDRS-R, RADS-2, MASC) (all $p < 0.001$; see Table 1) but did not significantly differ on age, gender, pubertal stage, IQ, and socioeconomic status.

3.1. Global and local graph metrics analyses

While there were no significant group differences in the global network properties ($p=0.3600$ for normalized average clustering coefficient, $p=0.4188$ for normalized characteristic path length, $p=0.7477$ for small-worldness), the local measure of node strength of the right caudate weighted by FA was significantly lower in the depressed subjects (difference $=0.0151$, $p<0.0001$, 2-sided *t*-test with unequal variances (uncorrected), resulting in $p<0.01$ after correcting for multiple comparisons across 90 AAL nodes). An example of streamlines going through the caudate in a representative MDD subject is shown in Fig. 1a.

GLM analysis of the FA-weighted right caudate node strength with diagnosis and age as covariates also revealed a statistically significant increment with age, across all subjects (0.0026 per year, $p=0.0366$) (Fig. 1b). None of the following measures showed significant correlation with the right caudate node strength in MDD subjects: clinician-rated depression symptom severity (CDRS-R; $r=-0.0136$, $p=0.9202$), self-reported depression symptom severity (RADS-2; $r=0.0295$, $p=0.8277$) and each of its subscales ($r=-0.0945$, $p=0.4846$ for Dysphoric Mood, $r=-0.1420$, $p=0.2921$ for Anhedonia/Negative Affect, $r=0.1242$, $p=0.3573$ for Negative Self-Evaluation, and $r=0.0218$, $p=0.8722$ for Somatic Complaints), anxiety symptom severity ($r=-0.1934$, $p=0.1571$), and total stress scores ($r=-0.1952$, $p=0.1493$).

Importantly, there were no significant differences in global mean FA or caudate volume between groups. Furthermore, removing the 10 medicated MDD subjects did not affect the finding of the between-group node strength difference (resulting in $p<0.0001$, uncorrected, or $p<0.01$ after correcting for multiple comparisons across 90 AAL nodes).

With the streamline count-weighted networks, no statistically significant differences were observed between the two groups, either for global or local network measures.

3.2. Edge-based analyses

Since NBS results depend on the choice of the primary threshold, we tested a range of thresholds (3.5, 3.6, 3.7… 6). The results of the edge-based FA-weighted connectome analysis using NBS are presented in Fig. 2. The highest primary threshold of 5.5 (resulting in p-value <0.001), at which the number of significantly different connections plateaued, revealed a right caudate-centered network comprising 13 nodes and 12 connections with lower FA in MDD (Fig. 3). In particular, connections between right caudate and frontal gyri (superior, middle, and inferior), between right caudate and insula, and between right caudate and anterior cingulate had significantly lower FA in adolescents with MDD. The connection that remained significant at the strictest primary threshold of 6 was between the right caudate and middle frontal gyrus (MFG).

The same right caudate-centered network comprising 13 nodes and 12 connections with lower FA in depressed adolescents was also detected after removing the 10 medicated MDD subjects (primary threshold 4.7, resulting in $p<0.001$). No statistically significant edge-based differences between the two groups were observed with the streamline count-weighted networks.

Our exploratory analysis revealed a significant *diagnosis* × *stress* interaction for the FA-based connectivity between right caudate and MFG (Fig. 4). In depressed subjects, the FA-based connectivity between the right caudate and MFG was negatively correlated with total stress (Fig. 4). In healthy subjects, on the other hand, there was no statistically significant correlation with stress. There were no statistically significant correlations with age ($r=0.1630$, $p=0.2256$), clinician- or self-rated depression ($r=-0.1226$, $p=0.3634$ for CDRS-R, $r=0.1045$, $p=0.4391$ for RADS-2) or anxiety scores ($r=-0.2336$, $p=0.0860$) in adolescents with MDD for this connection.

4. Discussion

This study reports DTI-based connectome-level differences in structural networks between depressed and well-matched healthy control adolescents. Our findings highlight the role of right caudate connectivity, in particular to frontal gyri, insula, and anterior cingulate, in this population.

We partially confirmed our original hypotheses:

1) There were statistically significant differences in local but not global network measures between MDD and HC adolescents.
2) The differences in local network measures involved frontolimbic connections.
3) The differences in network measures did not show statistically significant correlation with the depression severity scores.

Our findings greatly overlap with a recent study of adult MDD (Korgaonkar et al., 2014), in which the authors' NBS analysis demonstrated lowered structural connectivity within two distinct brain networks that are present in depression. The first network primarily involved the regions of the default mode network (specifically, the rostral anterior cingulate cortex and isthmus portion of the posterior cingulate cortex bilaterally and the right precuneus, in addition to the left cuneus and pericalcarine regions) and the second network comprised the frontal cortex, thalamus, and right caudate regions. Consistent with the results from our

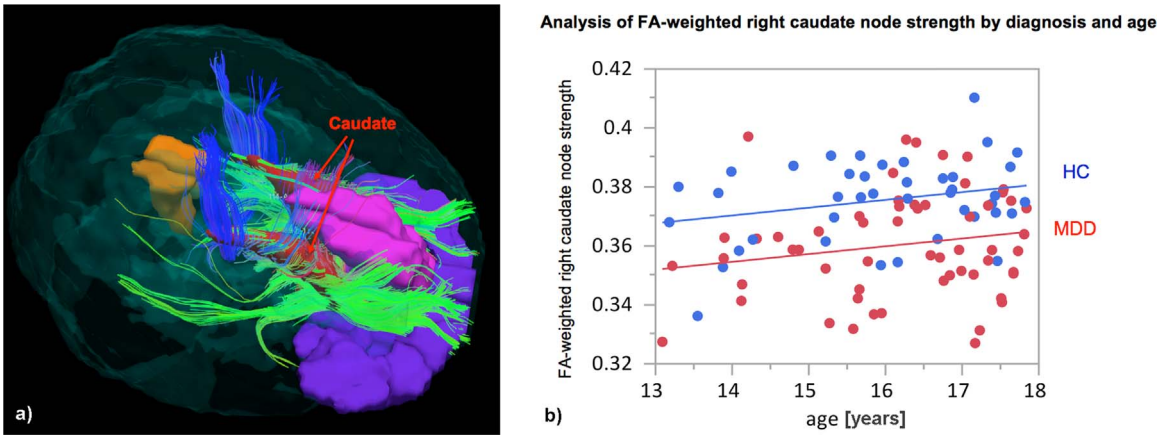

Fig. 1. a) Example of streamlines going through the caudate in an MDD subject. b) GLM analysis of the FA-weighted right caudate node strength with diagnosis and age as covariates. Increase of the node strength with age (0.0026 per year, $p=0.0366$) was observed.

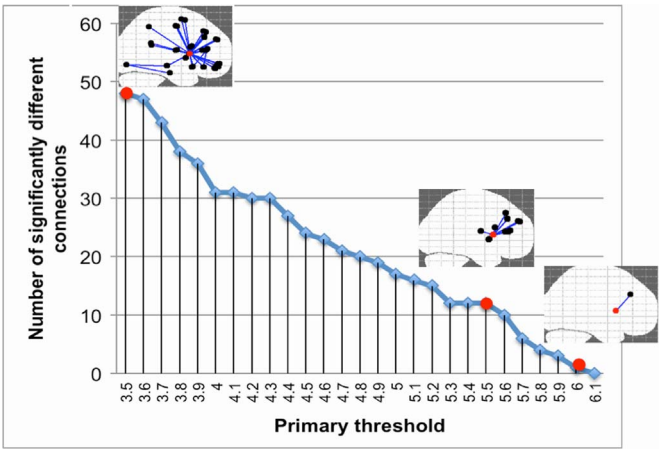

Fig. 2. The number of significantly different NBS-derived connections between depressed and healthy adolescents at different primary thresholds.

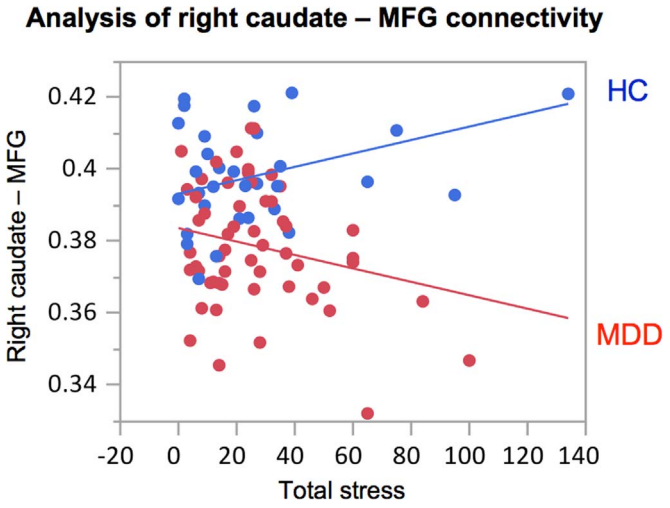

Fig. 4. GLM analysis of the FA-based connectivity between the right caudate and middle frontal gyrus (MFG) with diagnosis and diagnosis × total stress as covariates (the latter resulting in p=0.0080). Bivariate analysis with stress in MDD subjects resulted in a negative correlation, r=−0.3217, p=0.0156. Bivariate analysis with stress in healthy subjects resulted in a non-significant positive trend, r=0.2561, p=0.1643.

study, these two altered networks were observed in the context of an overall preservation of topology, meaning an absence of significant group differences for the global graph metrics. As in our study, the MDD-related abnormalities involved connections implicated in emotion and cognitive processing.

Our most notable finding is the right caudate region's potential central role in the network pathophysiology of adolescent MDD. The caudate is part of the striatum, and a critical component of the reward system, previously implicated in both adult (Pizzagalli et al., 2009) and adolescent MDD (Forbes and Dahl, 2012). It should be noted that in the AAL atlas, the caudate includes the nucleus accumbens (NAcc), which is thought to act as a motivation gateway between systems involved in emotion and motor control. The NAcc has previously been identified as a key center of the adult depression network and has been a target for deep brain stimulation in treatment-resistant depression (Schlaepfer et al.,

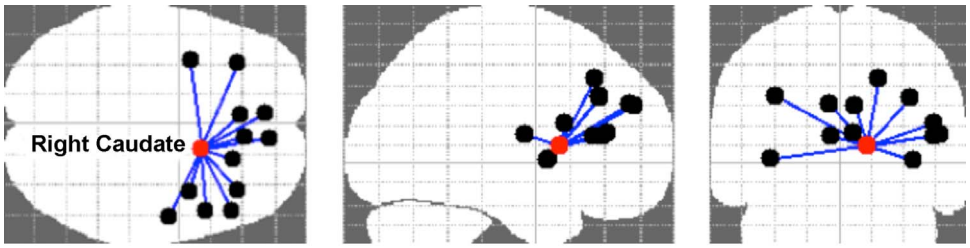

	Connection	Test statistic
1	Frontal_Sup_R to **Caudate_R**	5.68
2	Frontal_Mid_L to **Caudate_R**	5.64
3	Frontal_Mid_R to **Caudate_R**	6.07
4	Frontal_Inf_Oper_R to **Caudate_R**	5.81
5	Frontal_Inf_Tri_R to **Caudate_R**	5.96
6	Rolandic_Oper_R to **Caudate_R**	5.75
7	Frontal_Sup_Medial_L to **Caudate_R**	5.59
8	Frontal_Sup_Medial_R to **Caudate_R**	5.97
9	Insula_L to **Caudate_R**	5.57
10	Insula_R to **Caudate_R**	5.61
11	Cingulate_Ant_L to **Caudate_R**	5.63
12	Cingulate_Ant_R to **Caudate_R**	5.71

Fig. 3. NBS result at primary threshold 5.5, alpha threshold p=0.001 (the resulting p-value < 0.001) revealing a right caudate-centered network comprising 13 nodes and 12 connections with lower FA in adolescents with MDD. Abbreviations: R/L: right/left; Frontal_Sup: superior frontal gyrus, dorsolateral; Frontal_Mid: middle frontal gyrus; Frontal_Inf_Oper: inferior frontal gyrus, opercular part; Frontal_Inf_Tri_R: inferior frontal gyrus, triangular part; Rolandic_Oper: rolandic operculum; Frontal_Sup_Medial_L: superior frontal gyrus, medial; Cingulate_Ant: anterior cingulate and paracingulate gyri.

2014). Altered and stably low reward function has been previously found in adolescent depression using fMRI studies (Forbes and Dahl, 2012), with a pattern of low striatal response and high medial prefrontal response to reward, potentially due to disrupted balance of corticostriatal circuit function. For example, in a study of children and adolescents with and without MDD, the participants completed an fMRI task involving monetary reward and a self-reported rating of affect in their real world environments through a four-day cell-phone-based assessment (Forbes et al., 2009). Youth with MDD exhibited less striatal response than healthy controls during reward anticipation and reward outcome, but more response in dorsolateral and medial prefrontal cortex. Furthermore, diminished activation in the caudate was correlated with lower subjective positive affect in natural environments, particularly within the depressed group.

In our study, contrary to our expectations, structural connectivity of the right caudate was not significantly correlated with depression scores or anhedonia scores when only depressed teens were analyzed. The RADS-2 standard scores and empirically derived clinical cutoff score provide an indication of the clinical severity of the individual's depressive symptoms. This 30-item self-report measures the four basic dimensions of depression: Dysphoric Mood, Anhedonia/Negative Affect, Negative Self-Evaluation, and Somatic Complaints, whereas the depression total score represents the overall severity of depressive symptomatology. The absence of the significant correlation may be due to the uneven distribution and limited range of the scores within the depressed group.

Given that adolescence is a time of ongoing brain maturation, the pathophysiology of adolescent depression needs to be considered in the context of development. Our results demonstrated a positive correlation of the right caudate node strength with age (Fig. 1b). This is consistent with the finding that the fibers connecting striatum to prefrontal regions, which were identified in our study, continue to mature throughout adolescence (Asato et al., 2010). While the effect size of age on the node strength did not differ between the groups, there was an offset that made the right caudate node strength in MDD appear underdeveloped compared to controls (Fig. 1b).

In our NBS analysis, the connection that was detected robustly even at the strictest primary threshold was between the right caudate and middle frontal gyrus (MFG) (Fig. 2). The MFG makes up about one-third of the frontal lobe and encompasses Brodmann areas 9, 10, and 46. Brodmann area 46 and parts of area 9 roughly corresponds to the dorsolateral prefrontal cortex (DLPFC), which plays a role in working memory, attentional modulation, and affect regulation (Pavuluri et al., 2005). DLPFC is connected to the orbitofrontal cortex, as well as to the ACC, thalamus, hippocampus, caudate, and other brain areas, and it has been a target of transcranial magnetic stimulation to treat treatment-resistant depression (Chen et al., 2013). Brodmann area 10 is the largest and one of the least well understood cytoarchitectonic area in the human brain; it is connected with the limbic system by the uncinate fasciculus and may be involved in working memory, episodic memory retrieval, and attending to one's own emotions and mental states or those of other agents (Gilbert et al., 2006). A large and growing body of research implicates the ventromedial PFC and dorsolateral PFC (DLPFC) (which includes portions of MFG) as key neural substrates underlying adult depression (Koenigs and Grafman, 2009). Functional imaging studies associate depression with opposite patterns of activity in these areas: hypoactivity in DLPFC but hyperactivity in ventromedial PFC. Our fronto-caudal structural hypoconnectivity results are most likely driven by the DLPFC and not ventromedial PFC that is located below MFG or dorsal portions of MFG that were not connected by many streamlines to the caudate (Supplementary Fig. S2).

We would like to mention at this point that, in general, a direct comparison of neuroimaging-based structural and functional findings is non-trivial. In addition to the fact that the exact relationship between functional and structural findings might not be straightforward for methodological reasons (Damoiseaux and Greicius, 2009), functional hyperactivity or hyperconnectivity, for example, could in theory be either compensative or pathologic (Bi and He, 2014).

Stressful life events are linked to the mental health of adults and adolescents, and adolescents can be particularly vulnerable to stress (Hammen, 2005). Our study revealed a significant diagnosis × stress interaction for the right caudate–MFG connection (Fig. 4). Specifically, there was a significant negative correlation between right caudate-MFG connectivity strength and number of stressful life events in depressed subjects but a non-significant relationship in the HC. One possible interpretation is that stressful events only had a negative effect on this connection if the subject was already predisposed or diagnosed with depression and had lower connectivity within these white matter fibers.

Several methodological limitations need to be taken into account when interpreting our findings. First, a DTI-based deterministic tractography method was employed in this work to reconstruct structural brain networks. Although DTI-based methods are the most widely spread tractography methods, they have a limited capacity for resolving the fiber crossing issue and may result in misleading information about fiber tracts orientation (Farquharson et al., 2013). Thus, high-order reconstruction methods should be favored such as High Angular Resolution Diffusion Imaging (HARDI) diffusion models that are considered capable of resolving complex fiber crossings (Tuch et al., 2002). However, these methods require longer acquisition times. Moreover, even these most sophisticated tractography methods do not consistently show superior sensitivity and specificity (Thomas et al., 2014). Second, while the most widely used AAL atlas was utilized in this study, it is known that node definition by different parcellations might result in different properties of brain networks, especially due to the effects of spatial scale (De Reus and van den Heuvel, 2013). Therefore, graph analyses at several parcellation scales are encouraged in the future to provide more comprehensive information on the topological differences of structural brain networks in adolescent MDD. Third, tractography streamlines should not be understood as a quantitative estimate of white matter “connection strength” between the brain parcels (Jones et al., 2013). While these values can serve as “best possible guesses” for connectivity strength in the absence of any further information, one needs to keep in mind the huge uncertainties (variances) attached to them and that to date, it is not possible to reliably estimate the number of axonal projections from tractography. When a between-group difference is observed in tractography results, the only thing that can be inferred is that there is a difference in our ability to form a continuous path through the data field – the rest is modeling assumption (Jones et al., 2013). Biological origins of differences in both, streamline count and FA values, can be manifold and should be interpreted with caution.

In spite of the aforementioned limitations, tractography is central in structural connectivity studies, as it is currently the only non-invasive technique to obtain information about brain wiring. Our streamline count-weighted networks did not reveal any significant results in the depressed adolescents compared to controls. However, when we used the connecting streamlines between each pair of nodes as a mask, within which we calculated the average FA and used it as edge weights, pronounced between-group differences were detected. One of the strengths of our study is that we compared the connectomes on both global and local (at the node and edge) levels, two complementary ways of analysis, and applied a conservative multiplicity correction for both local and global measures (Meskaldji et al., 2013).

In previous research, by comparing FA within the white matter pathways yielded by tractography, Cullen and colleagues found that adolescents with MDD had lower FA in the tract connecting subgenual ACC to amygdala in the right hemisphere (Cullen et al., 2010). The hemispheric lateralization and location of their finding are in

partial agreement with our results. Previously, in the sample largely overlapping with the one in this paper, it was also found that adolescents with depression had significantly lower FA and higher radial diffusivity (RD) in the bilateral uncinate fasciculus (LeWinn et al., 2014). Tract-based spatial statistics (TBSS) additionally revealed lower FA values in the white matter associated with the limbic-cortical-striatal-thalamic circuit, corpus callosum, and anterior and superior corona radiata. In the present paper, we applied the novel connectome-based approach that has not been applied to depressed teens before, which produced congruent but complementary results to the LeWinn et al. (2014) study. In particular, the network-level analyses performed by us in this study allowed us to detect abnormal local network properties and a subnetwork of lower FA-based connectivity in depressed subjects, which demonstrates that adolescent MDD affects the brain at the network level. Another novel aspect of our study is the analysis of the Stressful Life Events data in relation to the brain network differences between depressed adolescents and healthy controls, which has not been explored before.

Based on our results, we would like to suggest two etiological models involving disrupted right caudate connectivity (Fig. 5). The links in the models are supported by our results, whereas the directions of causality represented by arrows are inferred by us based on the following logical considerations:

a) **Model involving right caudate connectivity.**
Given the relatively recent onset of depression in our sample, this model suggests that reduced structural connectivity of the right caudate could be a risk factor or even the underlying mechanism of adolescent MDD. White matter provides a means for electrochemical signaling across brain networks, thus, abnormal white matter microstructure within the afferent connections of the right caudate would hinder this region's proper function. In alignment with this causal assumption, Huang et al. showed that healthy adolescents at familial risk for unipolar depression had lower FA in a series of white matter tracts, suggesting that this might serve as a vulnerability marker for the illness (Huang et al., 2011). In this model, age can only have a causal role in its positive association with the node strength.

b) **Model involving right caudate–MFG connectivity.**
In this model, diagnosis plays a moderator role. Reduced connectivity between right caudate and MFG gives rise to adolescent depression, which, in turn, moderates the effect stressful events have on the connectivity between these two regions. This model highlights the vulnerability of adolescents predisposed to or diagnosed with MDD to stressful events and offers an alternative to the previously suggested stress-reward dysfunction-adolescent depression models (Auerbach et al., 2014).

It is also plausible that there is another variable (e.g., neurotransmitter levels) that causes the disruption of the right caudate connectivity with MFG and other regions, and, subsequently, causes the onset of depression, in which case the connectivity would play a role of a mediator. For example, a preliminary MR spectroscopy study of adolescents with major depression showed significantly elevated concentrations of choline and creatine, however, in the left, not right caudate (Gabbay et al., 2007). Choline/creatine ratio in the right caudate was significantly increased in depressed adults in another study (Li et al., 2016). More complex and bidirectional interactions are also plausible. Further investigations are needed to test the suggested causal links and possible mediations. We also suggest that future research directions include: i) evaluating robustness of the reported between-group network differences using different parcellation schemes, ii) comparing networks of medicated adolescents with MDD and unmedicated adolescents with MDD in larger samples, and iii) studying pre- versus post-treatment differences in structural connectivity of the caudate in depressed teens.

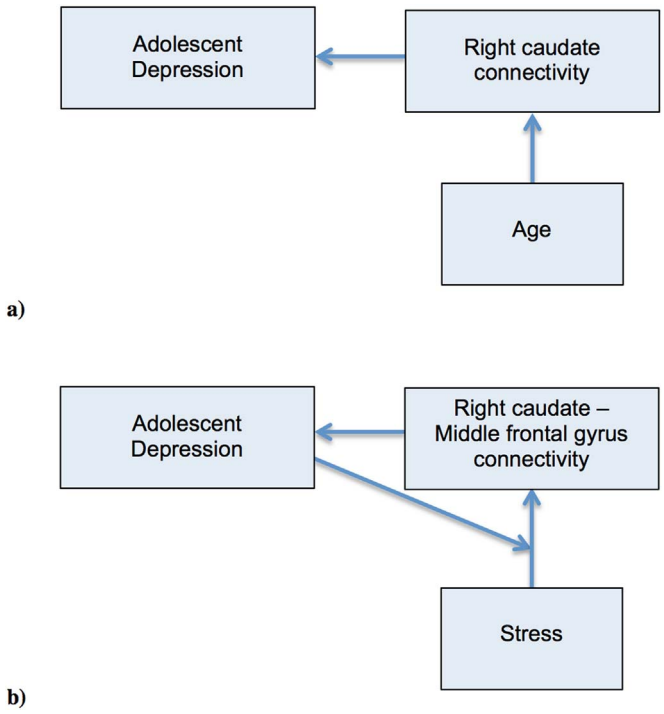

Fig. 5. Two etiological models involving disrupted right caudate connectivity are suggested. The links in the models are supported by our results, whereas the arrows are inferred by us based on logical considerations.

5. Conclusions

In this cross-sectional study we compared adolescents with major depressive disorder and healthy controls to determine if white matter brain networks differ between the two groups. The NBS-derived cluster of lower FA-based connectivity in depressed subjects was centered on the right caudate, providing empirical support for the pivotal role of the reward center in the pathophysiology of adolescent depression. We also observed that adolescents with major depressive disorder showed a significant negative correlation between right caudate–MFG connectivity and total stress, whereas the healthy controls did not exhibit such a relationship. Knowledge of the differences in network topology and results of bivariate analyses allowed us to suggest models of dysfunctional processes underlying adolescent depression.

In summary, DTI-based connectome analysis allowed us to investigate neurobiological abnormalities associated with adolescent major depressive disorder in vivo. We believe that our findings will help better understand the neural system abnormalities subserving this disorder.

Appendix A. Supplementary material

Supplementary data associated with this article can be found in the online version at http://dx.doi.org/10.1016/j.jad.2016.09.013.

References

Asato, M.R., Terwilliger, R., Woo, J., Luna, B., 2010. White matter development in adolescence: a DTI study. Cereb. Cortex 20, 2122–2131.
Auerbach, R.P., Admon, R., Pizzagalli, D.A., 2014. Adolescent depression: stress and reward dysfunction. Harv. Rev. Psychiatry 22 (3), 139–148.
Bessette, K.L., Nave, A.M., Caprihan, A., Stevens, M.C., 2013. White matter abnormalities in adolescents with major depressive disorder. Brain Imaging Behav. 8 (4), 531–541.

Bi, Y., He, Y., 2014. Connectomics reveals faulty wiring patterns for depressed brain. Biol. Psychiatry 76, 515–516.
Casey, B.J., Getz, S., Galvan, A., 2008. The adolescent brain. Dev. Rev. 28, 62–77.
Chen, J., Zhou, C., Wu, B., Wang, Y., Li, Q., Wei, Y., Yang, D., Mu, J., Zhu, D., Zou, D., Xie, P., 2013. Left versus right repetitive transcranial magnetic stimulation in treating major depression: a meta-analysis of randomised controlled trials. Psychiatry Res. 210, 1260–1264.
Cox, G.R., Callahan, P., Churchill, R., Hunot, V., Merry, S.N., Parker, A.G., Hetrick, S.E., 2014. Psychological therapies versus antidepressant medication, alone and in combination for depression in children and adolescents. In: Cochrane Database of Systematic Reviews. John Wiley & Sons, Ltd.
Cullen, K.R., Klimes-Dougan, B., Muetzel, R., Mueller, B.A., Camchong, J., Houri, A., Kurma, S., Lim, K.O., 2010. Altered white matter microstructure in adolescents with major depression: a preliminary study. J. Am. Acad. Child Adolesc. Psychiatry 49, 173–183.
Damoiseaux, J.S., Greicius, M.D., 2009. Greater than the sum of its parts: a review of studies combining structural connectivity and resting-state functional connectivity. Brain Struct. Funct. 213, 525–533.
De Reus, M.A., van den Heuvel, M.P., 2013. The parcellation-based connectome: limitations and extensions. Neuroimage 80, 397–404.
Farquharson, S., Tournier, J.-D., Calamante, F., Fabinyi, G., Schneider-Kolsky, M., Jackson, G.D., Connelly, A., 2013. White matter fiber tractography: why we need to move beyond DTI. J. Neurosurg. 118, 1367–1377.
Forbes, E.E., Dahl, R.E., 2012. Research review: altered reward function in adolescent depression: what, when and how? J. Child Psychol. Psychiatry 53, 3–15.
Forbes, E.E., Hariri, A.R., Martin, S.L., Silk, J.S., Moyles, D.L., Fisher, P.M., Brown, S.M., Ryan, N.D., Birmaher, B., Axelson, D.A., Dahl, R.E., 2009. Altered striatal activation predicting real-world positive affect in adolescent major depressive disorder. Am. J. Psychiatry 166, 64–73.
Gabbay, V., Hess, D.A., Liu, S., Babb, J.S., Klein, R.G., Gonen, O., 2007. Lateralized caudate metabolic abnormalities in adolescent major depressive disorder: a proton MR spectroscopy study. Am. J. Psychiatry 164 (12), 1881–1889.
Gilbert, S.J., Spengler, S., Simons, J.S., Steele, J.D., Lawrie, S.M., Frith, C.D., Burgess, P. W., 2006. Functional specialization within rostral prefrontal cortex (area 10): a meta-analysis. J. Cogn. Neurosci. 18, 932–948.
Griffa, A., Baumann, P.S., Thiran, J.P., Hagmann, P., 2013. Structural connectomics in brain diseases. Neuroimage 80, 515–526.
Hagmann, P., Kurant, M., Gigandet, X., Thiran, P., Wedeen, V.J., Meuli, R., Thiran, J.-P., 2007. Mapping human whole-brain structural networks with diffusion MRI. PLoS One 2, e597.
Hammen, C., 2005. Stress and depression. Annu. Rev. Clin. Psychol. 1, 293–319.
Huang, H., Fan, X., Williamson, D.E., Rao, U., 2011. White matter changes in healthy adolescents at familial risk for unipolar depression: a diffusion tensor imaging study. Neuropsychopharmacology 36, 684–691.
Jenkinson, M., Bannister, P., Brady, M., Smith, S., 2002. Improved optimization for the robust and accurate linear registration and motion correction of brain images. Neuroimage 17 (2), 825–841.
Jin, C., Gao, C., Chen, C., Ma, S., Netra, R., Wang, Y., Zhang, M., Li, D., 2011. A preliminary study of the dysregulation of the resting networks in first-episode medication-naive adolescent depression. Neurosci. Lett. 503, 105–109.
Jones, D.K., Knösche, T.R., Turner, R., 2013. White matter integrity, fiber count, and other fallacies: the do's and don'ts of diffusion MRI. Neuroimage 73, 239–254.
Koenigs, M., Grafman, J., 2009. The functional neuroanatomy of depression: distinct roles for ventromedial and dorsolateral prefrontal cortex. Behav. Brain Res. 201, 239–243.
Korgaonkar, M.S., Fornito, A., Williams, L.M., Grieve, S.M., 2014. Abnormal structural networks characterize major depressive disorder: a connectome analysis. Biol. Psychiatry 76, 567–574.
LeWinn, K.Z., Connolly, C.G., Wu, J., Drahos, M., Hoeft, F., Ho, T.C., Simmons, A.N., Yang, T.T., 2014. White matter correlates of adolescent depression: structural evidence for frontolimbic disconnectivity. J. Am. Acad. Child Adolesc. Psychiatry 53, 899–909.
Li Y., Jakary A., Gillung E., Eisendrath S., Nelson S.J., Mukherjee P. and Luks T., Evaluating metabolites in patients with major depressive disorder who received mindfulness-based cognitive therapy and healthy controls using short echo MRSI at 7 Tesla, *MAGMA* 29, 2016, 523–533.
March, J.S., Parker, J.D.A., Sullivan, K., Stallings, P., Conners, C.K., 1997. The multidimensional anxiety scale for children (MASC): factor structure, reliability, and validity. J. Am. Acad. Child Adolesc. Psychiatry 36, 554–565.
Meskaldji, D.E., Fischi-Gomez, E., Griffa, A., Hagmann, P., Morgenthaler, S., Thiran, J. P., 2013. Comparing connectomes across subjects and populations at different scales. Neuroimage 80, 416–425.
Moldrich, R.X., Pannek, K., Hoch, R., Rubenstein, J.L., Kurniawan, N.D., Richards, L.J., 2010. Comparative mouse brain tractography of diffusion magnetic resonance imaging. Neuroimage 51 (3), 1027–1036.
Mori, S., Crain, B.J., Chacko, V.P., van Zijl, P.C., 1999. Three-dimensional tracking of axonal projections in the brain by magnetic resonance imaging. Ann. Neurol. 45, 265–269.
Naicker, K., Galambos, N.L., Zeng, Y., Senthilselvan, A., Colman, I., 2013. Social, demographic, and health outcomes in the 10 years following adolescent depression. J. Adolesc. Health 52 (5), 533–538.
Pavuluri, M.N., Herbener, E.S., Sweeney, J.A., 2005. Affect regulation: a systems neuroscience perspective. Neuropsychiatr. Dis. Treat. 1, 9–15.
Pizzagalli, D.A., Holmes, A.J., Dillon, D.G., Goetz, E.L., Birk, J.L., Bogdan, R., Dougherty, D.D., Iosifescu, D.V., Rauch, S.L., Fava, M., 2009. Reduced caudate and nucleus accumbens response to rewards in unmedicated individuals with major depressive disorder. Am. J. Psychiatry 166, 702–710.
Poznanski, E.O., Mokros, H.B., 1996. Children's Depression Rating Scale—Revised (CDRS-R). Western Psychological Services, Los Angeles.
Reynolds, W.M., 2002. RADS-2, Reynolds Adolescent Depression Scale: Professional Manual. Psychological Assessment Resources, Lutz, FL.
Rubinov, M., Sporns, O., 2010. Complex network measures of brain connectivity: uses and interpretations. Neuroimage 52, 1059–1069.
SAMHSA – Substance Abuse and Mental Health Services Administration, 2014. NSDUH Series H-49, HHS Publication No. SMA 14–4887.
Schlaepfer, T.E., Bewernick, B.H., Kayser, S., Hurlemann, R., Coenen, V.A., 2014. Deep brain stimulation of the human reward system for major depression—rationale, outcomes and outlook. Neuropsychopharmacology 39, 1303–1314.
Smith, S.M., Jenkinson, M., Woolrich, M.W., Beckmann, C.F., Behrens, T.E.J., Johansen-Berg, H., Bannister, P.R., De Luca, M., Drobnjak, I., Flitney, D.E., Niazy, R. K., Saunders, J., Vickers, J., Zhang, Y., De Stefano, N., Brady, J.M., Matthews, P.M., 2004. Advances in functional and structural MR image analysis and implementation as FSL. Neuroimage 23, 208–219.
Sporns, O., Tononi, G., Kötter, R., 2005. The human connectome: a structural description of the human brain. PLoS Comput. Biol. 1, e42.
Thomas, C., Ye, F.Q., Irfanoglu, M.O., Modi, P., Saleem, K.S., Leopold, D.A., Pierpaoli, C., 2014. Anatomical accuracy of brain connections derived from diffusion MRI tractography is inherently limited. Proc. Natl. Acad. Sci. USA 111, 16574–16579.
Tuch, D.S., Reese, T.G., Wiegell, M.R., Makris, N., Belliveau, J.W., Wedeen, V.J., 2002. High angular resolution diffusion imaging reveals intravoxel white matter fiber heterogeneity. Magn. Reson. Med. 48, 577–582.
Tymofiyeva, O., Hess, C.P., Xu, D., Barkovich, A.J., 2014. Structural MRI connectome in development: challenges of the changing brain. Br. J. Radiol. 87, 20140086.
Tzourio-Mazoyer, N., Landeau, B., Papathanassiou, D., Crivello, F., Etard, O., Delcroix, N., Mazoyer, B., Joliot, M., 2002. Automated anatomical labeling of activations in SPM using a macroscopic anatomical parcellation of the MNI MRI single subject brain. Neuroimage 15, 273–289.
Wang, R., Benner, T., Sorensen, A.G., Wedeen, V.J., 2007. Diffusion toolkit: a software package for diffusion imaging data processing and tractography. Proc. Int. Soc. Magn. Reson. Med., 3720.
Williamson, D.E., Birmaher, B., Ryan, N.D., Shiffrin, T.P., Lusky, J.A., Protopapa, J., Dahl, R.E., Brent, D.A., 2003. The stressful life events schedule for children and adolescents: development and validation. Psychiatry Res. 119, 225–241.
Zalesky, A., Fornito, A., Bullmore, E.T., 2010. Network-based statistic: identifying differences in brain networks. Neuroimage 53, 1197–1207.